EUROTeV-Report-2006-019

Power losses of a nominal CLIC beam in the ILC 20 mrad extraction line

A. Ferrari*

June 20, 2006

Abstract

Strong beam-beam effects at the interaction point of a high-energy e^+e^- linear collider such as CLIC lead to an emittance growth for the outgoing beams, as well as to the production of beamstrahlung photons and e^+e^- coherent pairs. In this paper, we consider a nominal CLIC beam with an energy of 1.5 TeV and we estimate the power losses due to the disrupted beam, the beamstrahlung photons and the e^+e^- coherent pairs along the 20 mrad extraction line considered for ILC, with scaled magnet settings. We show that such a design is not adapted for the CLIC conditions, in particular because of the too large amount of low-energy particles found in the disrupted beam and the coherent pairs.

*Uppsala University, Sweden

1 Introduction

In a high-energy e^+e^- linear collider, the beams must be focused to extremely small spot sizes in order to achieve high charge densities and, in turn, to reach the desired luminosity. Because of the extremely small transverse dimensions of the colliding beams, electrons and positrons experience very strong transverse electromagnetic fields at the interaction point. The subsequent bending of their trajectories leads to the emission of hard beamstrahlung photons, which can then turn into e^+e^- (coherent and incoherent) pairs. Because of the large angular divergence and energy spread of the disrupted beams, a careful design of the extraction lines must be performed in order to transport the outgoing beams and the beamstrahlung photons from the interaction point to their dumps, with as small losses as possible. Also, the extraction lines should be fully instrumented to measure the main properties of the outgoing beams.

The CLIC project aims at multi-TeV e^+e^- collisions [1, 2]. In order to keep the length of the machine reasonably short, the design accelerating gradient and RF frequency are respectively 150 MV/m and 30 GHz. The bunch spacing is only a few cm, which is far too short to allow head-on collisions. At CLIC, the most stringent constraints on the crossing angle are set by the multi-TeV operation [3]. For a center-of-mass energy of 3 TeV, the angular distribution of the e^+e^- coherent pairs is such that the crossing angle θ_c must be larger than 20 mrad to avoid activation of the last quadrupole of the incoming beam line. On the other hand, because of the crossing angle, synchrotron radiation is emitted by the incoming particles in the solenoid field, as well as in the final quadrupole of the incoming beam line, which leads to an increase of the spot size at the interaction point. However, this growth remains acceptable if $\theta_c \leq 20$ mrad. When combining the effects of the secondary background due to coherent pairs and of the luminosity loss due to synchrotron radiation, one finds that the optimal crossing angle for CLIC should be 20 mrad. In addition, with this value of θ_c one keeps the multi-bunch kick instabilities at an acceptable level (these instabilities are induced by the parasitic collisions between the incoming and outgoing bunches and they are enhanced by a vertical offset). When bunches are collided with a large crossing angle, a significant fraction of the luminosity can be lost. At CLIC, without further action, the luminosity would indeed be about 10 times smaller with $\theta_c = 20$ mrad than in the case of head-on collisions. Therefore, crab cavities must be used: by deflecting the head and the tail of each bunch in opposite horizontal directions upstream of the interaction point, they force the bunches to be perfectly aligned when they collide, which in turn allows to recover the luminosity.

The ILC project [4] aims at e^+e^- collisions with a center-of-mass energy from 500 GeV to 1 TeV. With the superconducting technology, lower acceleration frequencies are favoured. Therefore, the spacing between two consecutive bunches (about 100 m) becomes so large that multi-bunch kick instabilities do not occur at ILC and one is not forced to use a large crossing angle for the e^+e^- collisions. The main challenge with very small crossing angles is the extraction of the disrupted beam, which is achieved by sending the outgoing beam off-center in large superconducting quadrupoles or sextupoles. On the other hand,

for large crossing angles, one must deal with technical difficulties such as, for instance, large crab-crossing corrections, as well as with other complications due to the passage of the beams through the solenoid field of the surrounding detector. Two configurations are currently being studied in the ILC design: one with a small crossing angle (2 mrad) and one with a large crossing angle (20 mrad).

In a previous study, an estimation of the power losses in the ILC 20 mrad extraction line was performed for various configurations of a TeV linear collider [5]. In the case of a CLIC machine which is operated at 1 TeV with the same beam delivery system as in the nominal 3 TeV case, it was shown that the power losses in the extraction line were too large, mostly because of the long low-energy tails of the disrupted beam, which tend to be over-focused in the quadrupoles located just downstream of the interaction point. In this paper, we estimate the power losses along the same extraction line (with different magnet settings) in the case of a nominal CLIC machine, i.e. with a center-of-mass energy of 3 TeV. In Section 2, we review the incoming and outgoing beam distributions at the interaction point. Then, in Section 3, we perform particle tracking in the ILC 20 mrad extraction line and we make a detailed estimation of the power losses. In Section 4, we repeat the same analysis, but with modified magnet settings in order to lower the power losses. Finally, some conclusions are given in Section 5.

2 Incoming and outgoing beams at the interaction point

The incoming beam parameters of the nominal CLIC machine are given in Table 1. Knowing them, the disrupted beam distributions at the interaction point can be then obtained with the GUINEA-PIG code [6].

Parameter	Symbol	Value	Unit
Center-of-mass energy	E	3	TeV
Particles per bunch	N_b	2.56	10^9
Bunches per RF pulse	n	220	
Bunch spacing	Δt_b	0.267	ns
Repetition frequency	f	150	Hz
Primary beam power	P_b	20.4	MW
Horizontal normalized emittance	$(\beta\gamma)\epsilon_x$	660	nm.rad
Vertical normalized emittance	$(\beta\gamma)\epsilon_y$	10	nm.rad
Horizontal rms beam size	σ_x	60	nm
Vertical rms beam size	σ_y	0.7	nm
Rms bunch length	σ_z	30.8	μm
Peak luminosity	L	6.5	10^{34} cm^{-2} s^{-1}

Table 1: Incoming beam parameters of the nominal CLIC machine [7].

The transverse distributions of the CLIC disrupted beams are shown in Figure 1. Note that the double-peak shape of the x'-distributions is characteristic for collisions with flat beams. The strong beam-beam interactions lead to an increase of the angular divergence of the colliding beams, and therefore to a significant emittance growth at the interaction point (in both transverse directions).

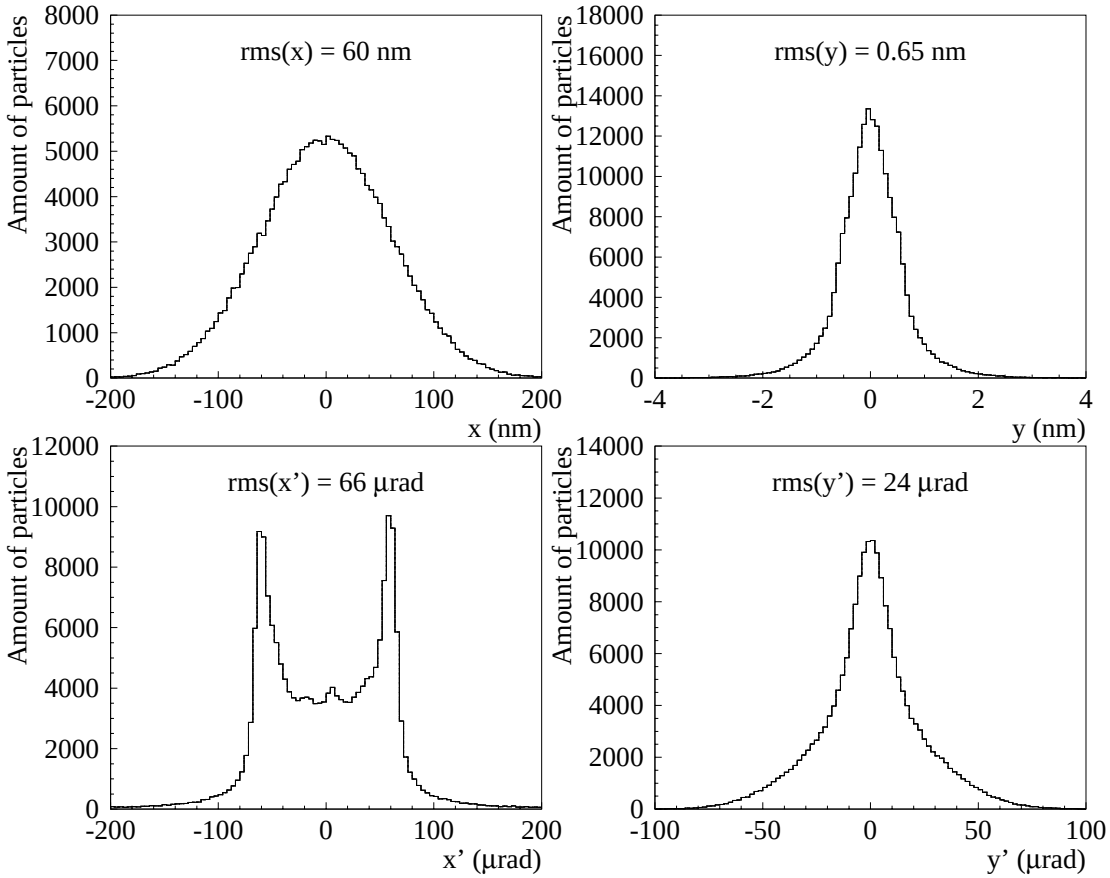

Figure 1: Transverse distributions of the disrupted beams at the interaction point of the nominal CLIC machine. Here, 10^5 macro-particles were used in the GUINEA-PIG simulation.

Figure 2 shows the energy spectrum of the CLIC disrupted beams at the interaction point. The long low-energy tails account for the emission of beamstrahlung photons during the bunch crossing. Simulations performed with GUINEA-PIG indicate that, in average, 1.1 beamstrahlung photons are emitted per incoming electron or positron. As for the beamstrahlung parameter δ_B (the average energy loss of each incoming beam through emission of photons), it is 16% at CLIC. The angular distributions of the outgoing beamstrahlung photons are shown in Figure 3.

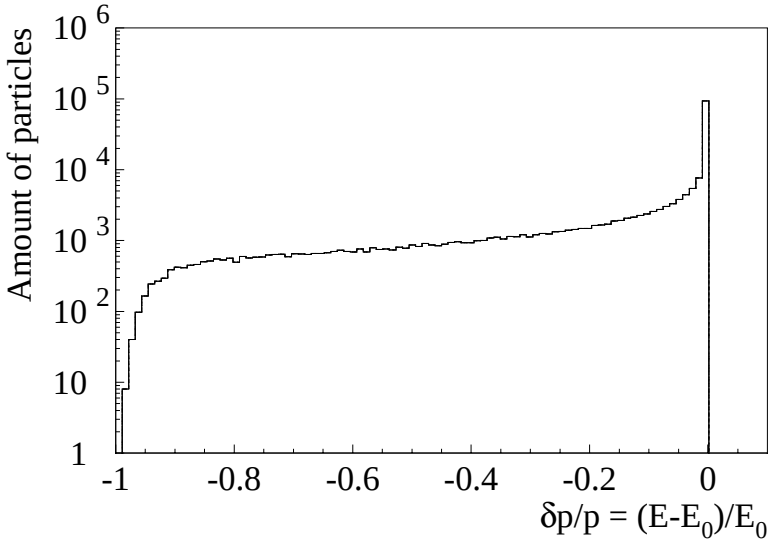

Figure 2: Energy spectrum of the disrupted beams at the interaction point of the nominal CLIC machine. Here, 10^5 macro-particles were used in the GUINEA-PIG simulation.

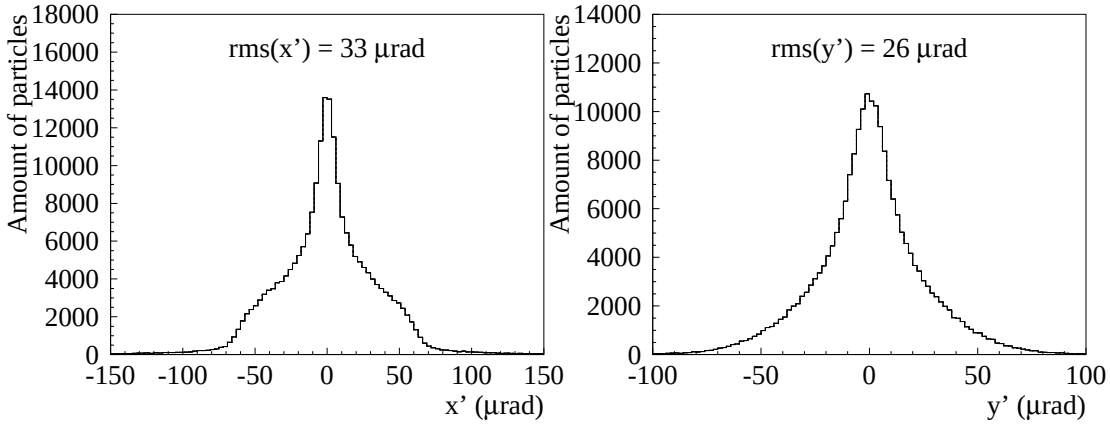

Figure 3: Angular distributions of the beamstrahlung photons at the interaction point of the nominal CLIC machine. Here, 10^5 macro-particles were used in the GUINEA-PIG simulation, which leads to 2.2×10^5 beamstrahlung photons when both outgoing directions are considered.

In the presence of a strong electromagnetic field, beamstrahlung photons can turn into e^+e^- coherent or incoherent pairs. The coherent pairs arise from the interaction of the beamstrahlung photons of one beam with the collective electromagnetic field of the other beam. The incoherent pairs result from the interaction of (real or virtual) photons of

one beam with particles from the other beam. Because of their low energy, the main concern with the incoherent pairs is how they contribute to the detector background, rather than the small amount of power deposited by a fraction of these low-energy pairs in the extraction line. In the following, we thus only focus on the e^+e^- coherent pairs, which carry significantly more energy. The probability associated to the e^+e^- coherent pair production depends essentially on the parameter Υ defined as [8]:

$$\Upsilon = \frac{5}{6} \frac{\gamma r_e^2 N_b}{\alpha \sigma_z \sigma_y (1 + \sigma_x/\sigma_y)}, \tag{1}$$

where $\alpha = 1/137$ and $r_e = 2.82 \times 10^{-15}$ m are respectively the fine-structure constant and the classical electron radius.

At CLIC, $\Upsilon \simeq 3.6$ and the expected number of e^+e^- coherent pairs, derived from GUINEA-PIG simulations, is 4.6×10^7 per bunch crossing. The transverse distributions of such pairs are shown in Figure 4. The electrons and positrons of the coherent pairs carry typically about 10% of the primary beam energy, as it is shown in Figure 5.

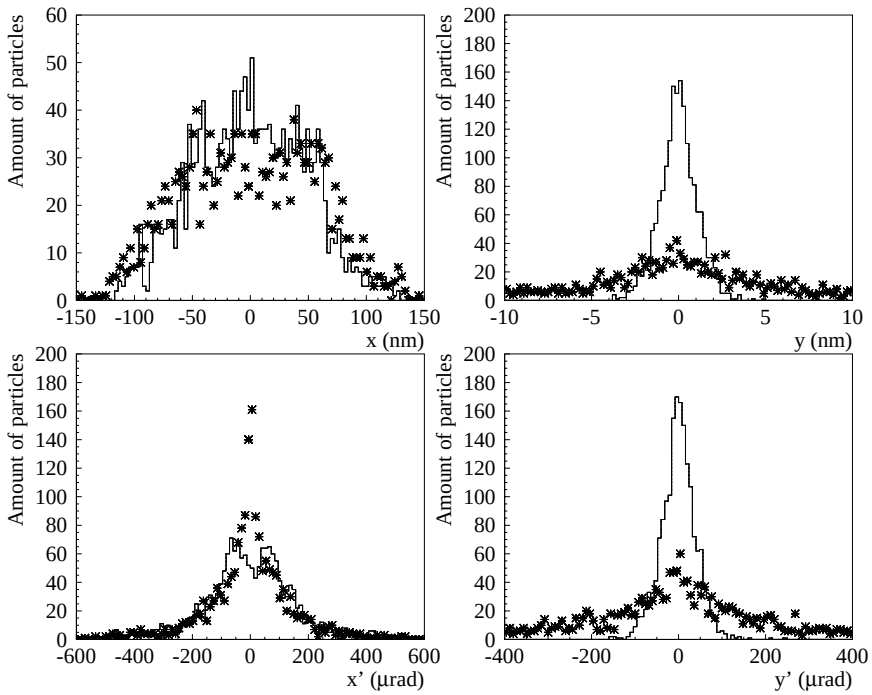

Figure 4: Transverse distributions of the e^+e^- coherent pairs at the interaction point of the nominal CLIC machine. Here, 10^5 macro-particles were used in the GUINEA-PIG simulation, which leads to 1.8×10^3 coherent pairs. Full lines correspond to particles that have the same charge as the disrupted beam, while stars correspond to the opposite charge.

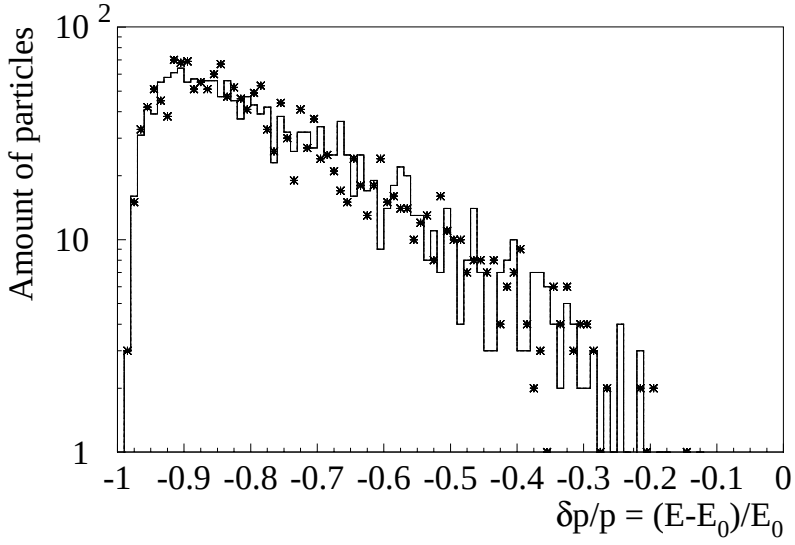

Figure 5: Energy spectrum of the e^+e^- coherent pairs at the interaction point of the nominal CLIC machine.

For the sake of simplicity, all outgoing beam distributions were produced with GUINEA-PIG assuming that the incoming beam have transverse Gaussian distributions. In reality, this is not the case, and tails should be taken into account. In this study however, we do not aim at calculating the power losses of a CLIC beam along the extraction line with a high degree of precision. We rather want to estimate the levels of deposited power due to the disrupted beam, the beamstrahlung photons and the coherent pairs in the various magnetic elements of the extraction line, in order to identify the limitations of the current ILC design for the CLIC operation.

3 Particle tracking in the ILC 20 mrad extraction line

At an e^+e^- linear collider with a 20 mrad crossing angle, one will use a dedicated line to transport the outgoing beams (together with the beamstrahlung photons) from the interaction point to their dump. In the present design of the ILC 20 mrad extraction line [9], the disrupted beams and the beamstrahlung photons all go through the same magnets to one shared dump. The optics consists of a DFDF quadruplet, followed by two vertical chicanes for energy and polarization measurements and a field-free region that allows the beam to grow naturally, with two round collimators located 200 m and 300 m downstream of the interaction point, with a radius of 8.8 cm and 13.2 cm respectively, in order to reduce the maximum beam size at the dump, see Figure 6. Note that the first quadrupoles of the ILC extraction line were chosen to be superconducting, thereby allowing to reach higher focusing gradients and to reduce their length, as compared to warm quadrupoles.

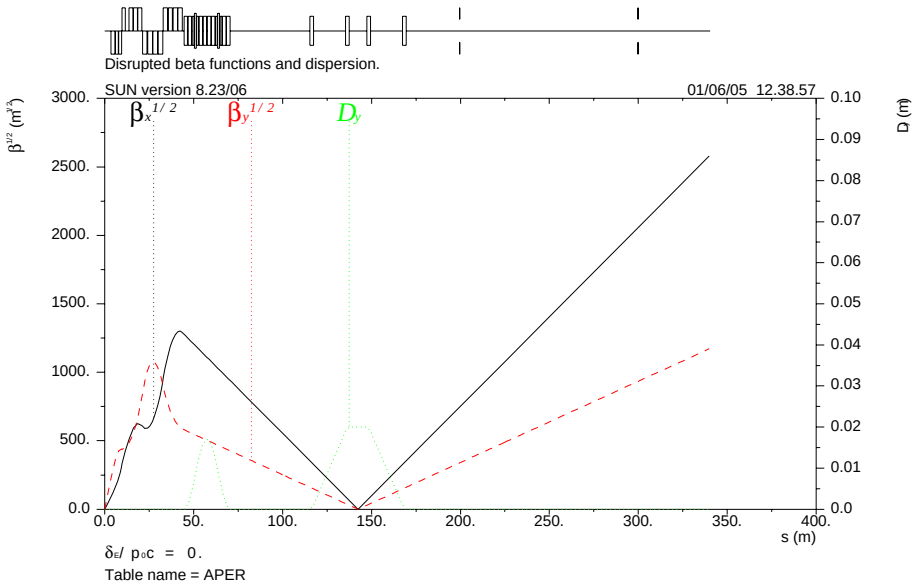

Figure 6: Betatron functions and vertical dispersion along the ILC extraction line with a 20 mrad crossing angle. This is an update of the lattice described in [9].

3.1 Power loss for the disrupted beams

The disrupted beam distributions of Figure 1 were tracked from the interaction point to the dump using DIMAD [10]. This program computes particle trajectories in a given beam line using the second order matrix formalism [11]. The DIMAD code was updated in order to handle very large energy spreads such as those found in the CLIC disrupted beams downstream of the interaction point. Here, a nominal beam energy of 1.5 TeV is used when setting the fields in all magnetic elements.

Using the number of lost particles in the extraction line, as well as their energy, one can calculate the total beam power loss with the following formula:

$$P_{loss} = 1.602 \times 10^{-10} \frac{N_b\, n\, E\, f}{N_{tracks}} \sum_{i=1}^{N_{loss}} \left(1 + \frac{\delta E_i}{E}\right). \qquad (2)$$

In this equation, N_b is the number of particles per bunch, n is the number of bunches per RF pulse, f is the repetition frequency (in Hz), E and $E_i = E + \delta E_i$ are respectively the nominal energy of the beam and the energy of the particle i (both in GeV), N_{tracks} and N_{lost} are respectively the number of tracked and lost particles. With these conventions, P_{loss} is expressed in Watts.

Particle tracking with DIMAD clearly shows that most of the disrupted beam losses come from the low-energy tail. The smaller a particle energy, the earlier it is lost in the extraction line. Indeed, electrons and positrons which have lost a large fraction of their initial energy through the emission of beamstrahlung photons tend to be over-focused

in the first quadrupoles of the extraction line and thus deposit a significant amount of power there. The particles that have a somewhat larger energy at the interaction point may still go through the quadrupoles without being lost, but their energy is still too low for a transmission through the vertical chicanes. Indeed, the 20 mrad extraction line only accepts the primary electrons/positrons with $E_i/E > 40\%$, see the left-hand plot of Figure 7. Note that the vertical line pattern is due to the structure of the DIMAD output, where losses are assigned to each element of the beam line, instead of being continuously distributed.

In order to better estimate the impact of the disrupted beam losses, the right-hand side plot of Figure 7 shows the loss density in all elements of the 20 mrad extraction line, upstream of the collimators. There, we have also estimated the total beam losses and the largest value of the loss density in the superconducting and warm quadrupoles, as well as in the bending magnets of the energy and polarimetry chicanes, see Table 2. As for the beam losses in the two round collimators, we find 87.8 kW in COLL1 and 11.4 kW in COLL2.

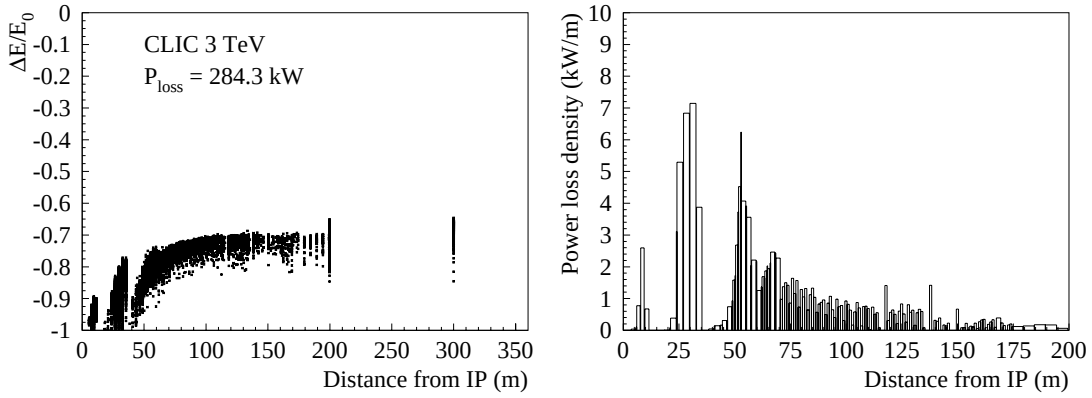

Figure 7: Relative energy spread of the lost particles as a function of the position of loss in the 20 mrad extraction line (left) and loss density upstream of the collimators (right), obtained when tracking the disrupted CLIC beams.

Magnetic elements	Total beam losses	Maximal loss density
SC Quadrupoles	6.5 kW	2.6 kW/m
Warm Quadrupoles	61.5 kW	7.1 kW/m
Energy Chicane Magnets	48.0 kW	4.5 kW/m
Polarimetry Chicane Magnets	0.8 kW	0.4 kW/m

Table 2: Total beam losses and maximal loss density in the first section of the 20 mrad extraction line (upstream of the collimators) for CLIC at 3 TeV.

3.2 Power loss for the beamstrahlung photons

In addition to the significant emittance growth at the interaction point, strong beam-beam effects also lead to the emission of beamstrahlung photons, which must then be transported to their dump with minimal losses along the extraction line. Since photons do not carry any electric charge, they are not affected by magnetic fields and follow straight trajectories, which are fully determined by their initial angle at the interaction point. As a result, one can treat them exactly as electrons/positrons traveling through field free regions. When tracking these beamstrahlung photons with DIMAD, one must assign their original position to $x = y = 0$, switch-off all magnetic elements along the extraction line and turn-off charged particle effects, such as synchrotron radiation. In addition, when tracking photons, one must make sure that all magnets are placed on the reference trajectory, which is defined by the nominal energy electron or positron beam. In other words, one needs to vertically misalign all elements inside the chicanes, so that the beamstrahlung photons go correctly through their aperture.

Using the number of lost photons in the extraction line, one then calculates the total beamstrahlung power loss with the following formula:

$$P_\gamma = 1.602 \times 10^{-10} \, \frac{N_\gamma \, n \, f}{N^\gamma_{tracks}} \, \sum_{i=1}^{N^\gamma_{loss}} E_{\gamma i}. \tag{3}$$

In this equation, N_γ is the number of beamstrahlung photons emitted by bunch crossing in a given direction (note that GUINEA-PIG produces photons along both outgoing beam directions) and $E_{\gamma i}$ is the energy of each lost photon.

We find that the power loss associated to the beamstrahlung photons remains negligible: $P_\gamma \simeq 55$ W. Also, our simulations with DIMAD indicate that beamstrahlung photon losses occur almost exclusively in the first round collimator. Located 200 m downstream of the interaction point, with a radius of 8.8 cm, COLL1 allows only beamstrahlung photons produced with an angle smaller than 0.44 mrad to pass through (this is chosen to limit the disrupted beam size to a 150 mm radius of the dump window).

3.3 Power loss for the coherent pairs

For a given disrupted beam direction, one runs two tracking simulations with DIMAD: one for the particles that have the same charge as the disrupted beam and one for the particles with the opposite charge. In the latter case, since DIMAD does not know the charge of the tracked particle, one must change the polarity of all magnetic elements and, in addition, make sure that all magnets are placed on the reference path defined by the nominal (undisrupted) beam. For this purpose, one must vertically misalign all elements inside the chicanes, so that the wrong-sign particles go correctly through them. However, the corresponding reduction of aperture remains of the order of a few percent only and thus does not significantly affect the losses.

About 80% of the particles coming from the coherent pairs do not reach the dump at the end of the extraction line. The left-hand side plot of Figure 8 shows that power losses mostly occur due to the over-focusing of low-energy particles in the quadrupoles: the lower the energy of the tracked particle, the sooner it is lost after the interaction point. This plot also indicates that the distribution of the power losses along the extraction line does not significantly depend on the particle charge. The right-hand side plot of Figure 8 shows that the power loss density (estimated for both electrons and positrons) in the quadrupoles is of the order of a kW/m, i.e. just a few times smaller than for the disrupted beam. At 3 TeV, the coherent pairs have a non-negligible contribution to the total power losses, especially in the first part of the extraction line, where the low-energy electrons and positrons tend to be over-focused by the quadrupoles.

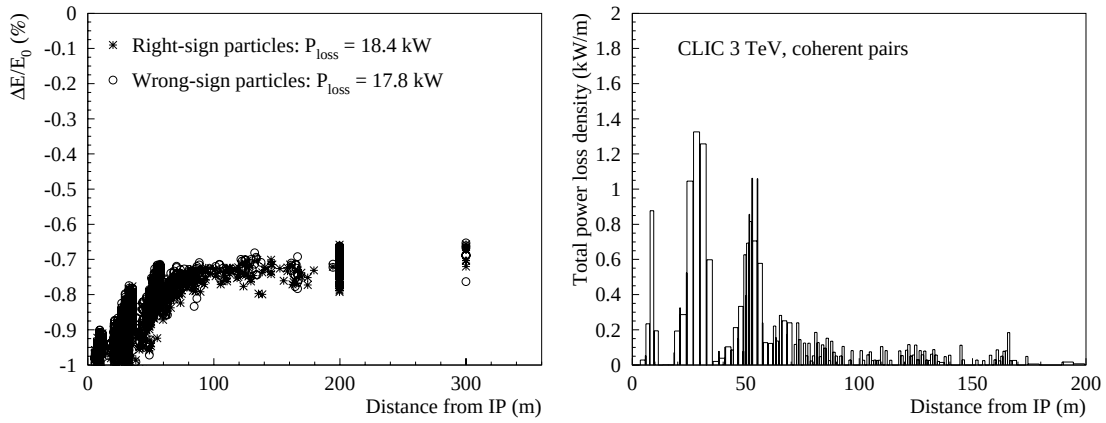

Figure 8: Relative energy spread of the lost particles as a function of the position of loss in the 20 mrad extraction line (left) and power loss density upstream of the collimators (right), obtained by tracking e^+e^- coherent pairs, in the nominal CLIC case.

4 Power losses versus magnet settings

With the default magnet settings, which are such that the normalized gradients of the quadrupoles and the bending angles of the dipoles are exactly the same at 1.5 TeV as they were at lower energies, the power losses of the CLIC beam along the ILC 20 mrad extraction line are by far too large. These losses are mostly resulting from the over-focusing of low-energy particles (the tails of the disrupted beam and the coherent pairs) in the quadrupoles. In this section, we investigate whether different magnet settings, which do not focus the low-energy particles too strongly, may allow to lower the power losses along the extraction line.

Let f_{QB} be the common scaling factor for all normalized gradients and bending angles along the 20 mrad extraction line. Scaling down the magnetic fields in all dipoles and quadrupoles by f_{QB} is equivalent to changing the central energy of the beam, thereby effectively reducing the total energy spread, which allows transmission of more particles. For the new central energy (i.e $f_{QB} \times 1.5$ TeV), the optics is the same as the optics for the original nominal energy. Figure 9 shows how the total power losses, associated to the disrupted beam and the coherent pairs, vary with f_{QB}. The magnet settings have no effect on the beamstrahlung photons.

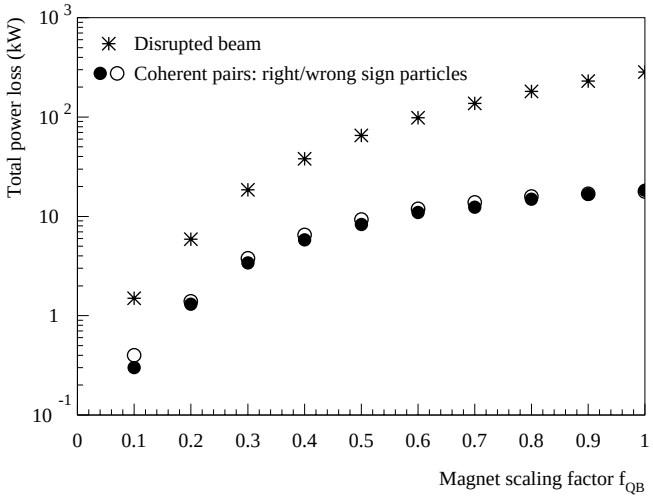

Figure 9: Total power losses in the 20 mrad extraction line with a 1.5 TeV CLIC beam, as a function of the common magnet scaling factor f_{QB}.

The smaller the normalized gradients and the bending angles, the smaller the power losses: indeed, less and less low-energy particles are over-focused in the first quadrupoles and hit the vacuum pipe when f_{QB} decreases. Meanwhile, particles with a high energy (close to the nominal one) experience a smaller force from the dipolar and quadrupolar magnetic fields and thus tend to have straighter trajectories. Since they are produced with a small angular divergence at the interaction point, they are likely to travel through the whole extraction line without hitting the vacuum pipe or the collimators, and thus reach the dump without having deposited their energy upstream.

Figure 10 gives more details about the power losses in various elements of the extraction line, namely the superconducting and warm quadrupoles (see the upper plots, on the left and right sides respectively), the bending magnets of the energy chicane (see the lower plot on the left side), as well as the two collimators (see the lower plot on the right side). The power deposited in the bending magnets of the polarimetry chicane is generally much smaller than in the other elements and was thus not plotted here.

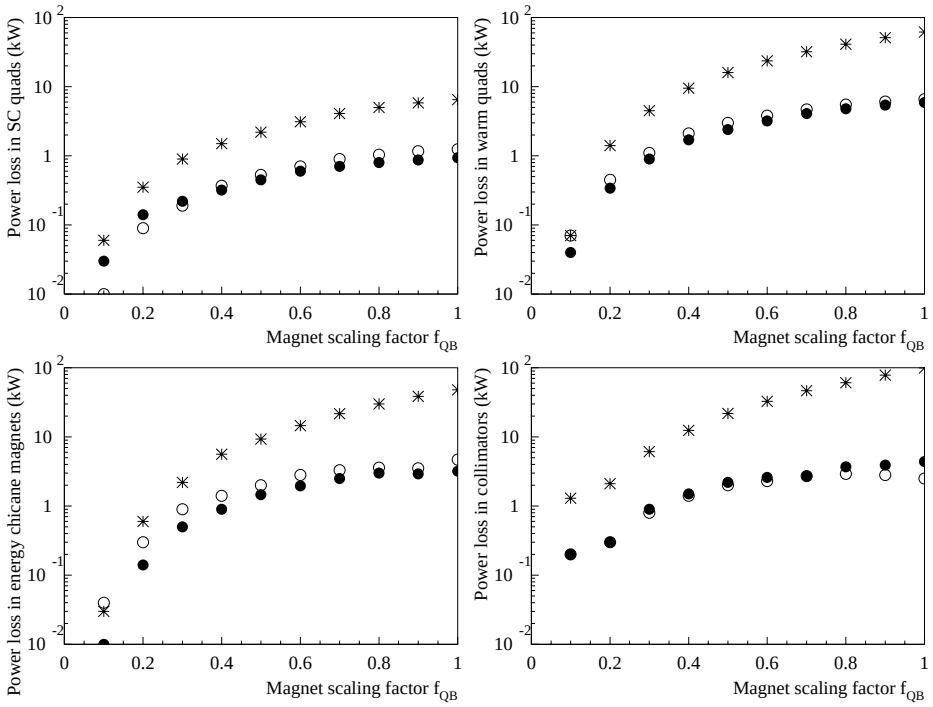

Figure 10: Power losses in various elements of the 20 mrad extraction line with a 1.5 TeV CLIC beam, as a function of the common magnet scaling factor f_{QB}. In all plots, the stars correspond to the disrupted beam, while the full and open circles correspond to the particles from the coherent pairs (the charge being respectively same as and opposite to the charge of the disrupted beam).

One should reduce the fields in all magnetic elements by at least a factor five to reach a reasonable level of losses with a 1.5 TeV CLIC beam in the 20 mrad extraction line. But, even so, the power deposited in the superconducting quadrupoles is still a few hundred Watts. Also, the optics of the extraction line at the nominal energy is destroyed when changing all magnetic fields in the dipoles and quadrupoles. In particular, the optics condition for a secondary focus point is no longer fulfilled at the nominal energy, which prevents from performing polarimetry measurements in the second vertical chicane. This is illustrated by Figure 11, where the transverse distributions of the disrupted beam are shown in two cases: $f_{QB} = 1$ and $f_{QB} = 0.2$. In the latter case, the gradients of the quadrupoles are too weak for a focus-to-focus transformation of the beam. Instead, one has roughly a focus-to-parallel transformation, where the x-distribution at the secondary focus point is similar to the x'-distribution at the interaction point. Beyond the scope of this paper, one should investigate alternative optics, still allowing a secondary focus point where the dispersion is large, but with low magnetic fields in the quadrupoles in order to ensure small beam losses.

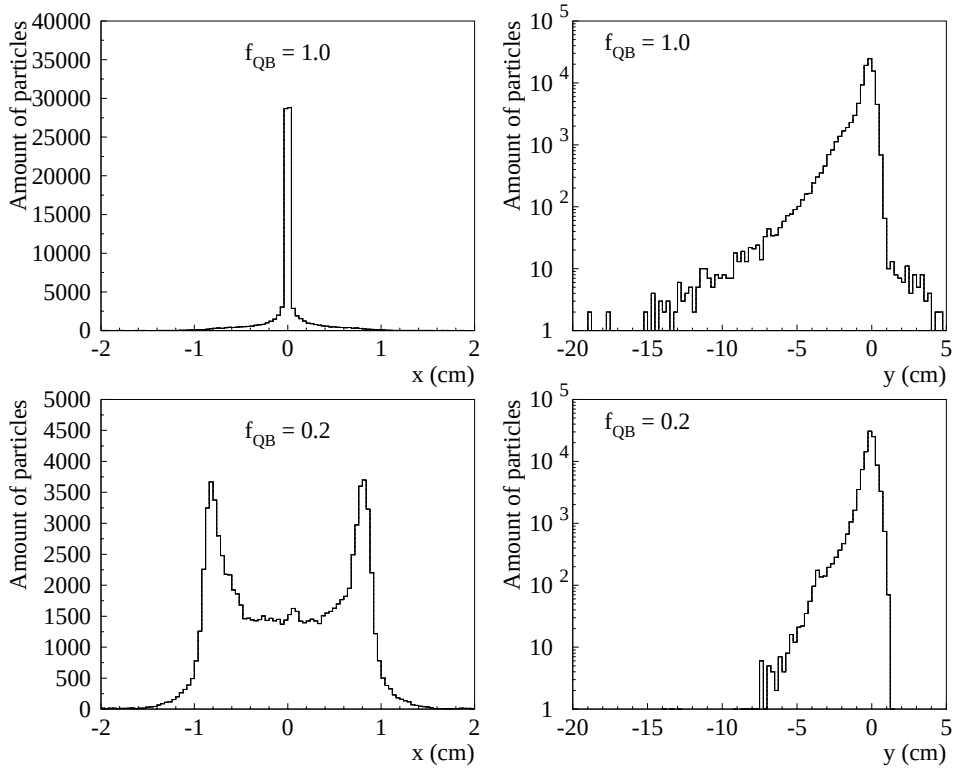

Figure 11: Transverse distributions of the CLIC disrupted beam at the secondary focus point, as obtained with $f_{QB} = 1$ (upper plots) and $f_{QB} = 0.2$ (lower plots).

Figure 12 shows a comparison of the transverse sizes of the disrupted beam at the dump, obtained with $f_{QB} = 1$ and $f_{QB} = 0.2$. In these plots, the dependence of the transverse position on the energy of the tracked particle is also visible. As expected, the spot size at the dump is larger for the low-energy particles ($\delta p/p < -0.6$ typically) than for the high-energy particles, and this result does not significantly depend on f_{QB}. In the high-energy part of the spectrum, note that one obtains a similar spot size with $f_{QB} = 1.0$ and $f_{QB} = 0.2$. One major difference is that one finds almost no particle with $\delta p/p > -0.2$ when $f_{QB} = 1.0$. These high-energy particles are not lost along the extraction line but their energy decreases due to synchrotron radiation in the strong magnetic fields of the quadrupoles and dipoles. When one sets $f_{QB} = 0.2$, these magnetic fields are weaker and, in turn, less energy is lost through synchrotron radiation. Note that DIMAD does not track the photons that are produced through synchrotron radiation in the magnetic elements of the extraction line, although they may hit the vacuum chamber or a magnet and contribute to the power losses.

Figure 13 shows a comparison of the transverse distributions of the undisrupted CLIC beam at the dump, obtained with $f_{QB} = 1$ and $f_{QB} = 0.2$. The spot size has roughly the same area in both cases.

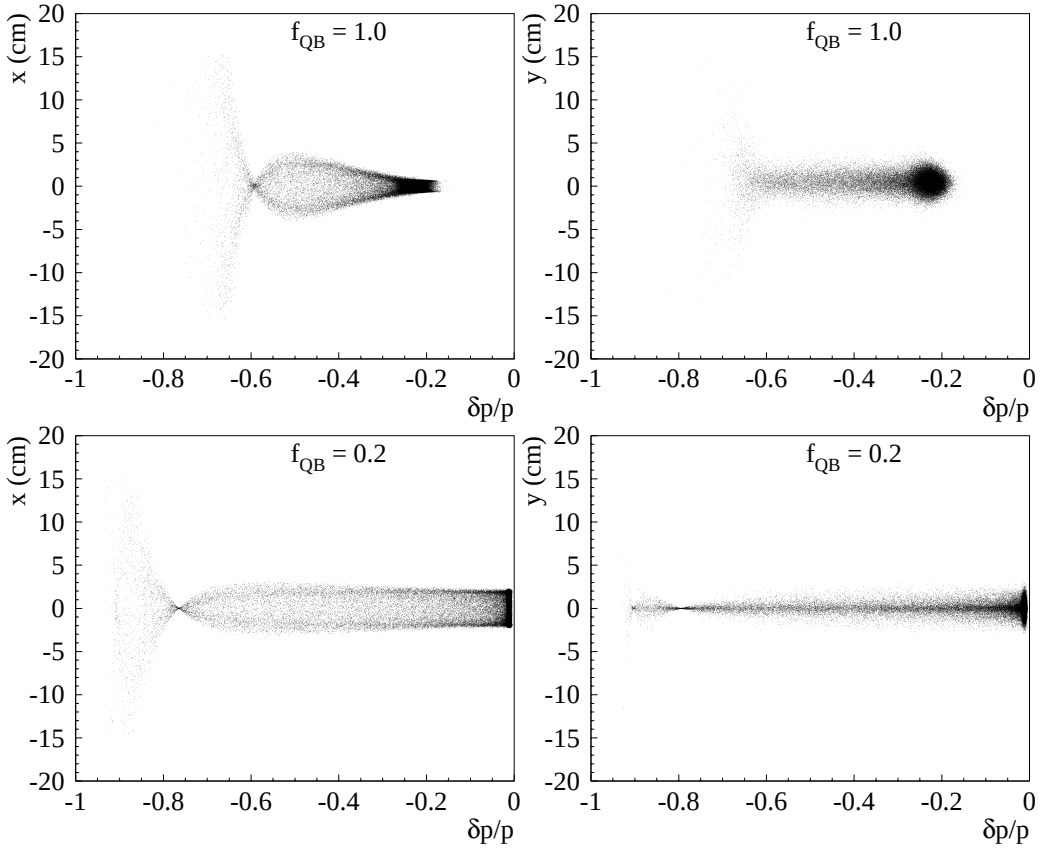

Figure 12: Transverse position of the particles in the CLIC disrupted beam as a function of their energy, obtained at the dump with two different magnet settings: $f_{QB} = 1$ (upper plots) and $f_{QB} = 0.2$ (lower plots).

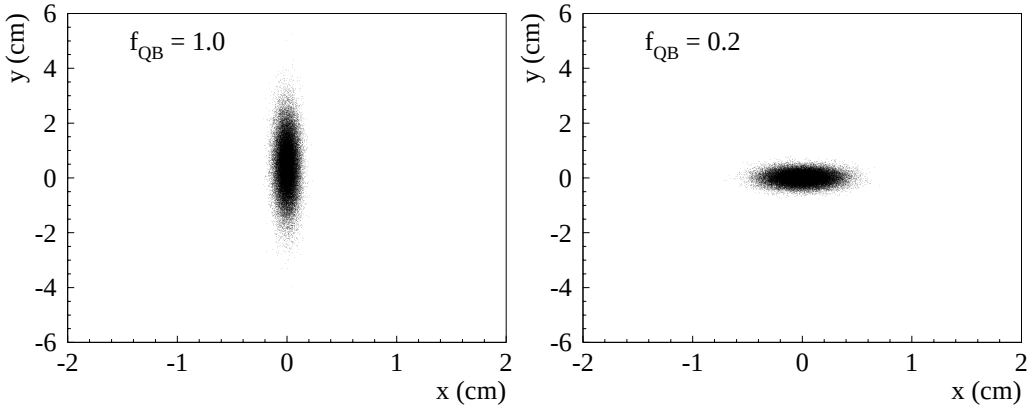

Figure 13: Transverse distribution of the CLIC undisrupted beam at the dump, with $f_{QB} = 1$ (left) and $f_{QB} = 0.2$ (right).

In order to transport a nominal CLIC beam to its dump through a 20 mrad extraction line, while being also able to perform measurements, one must consider a new post-collision optics, which will be discussed in future reports. Another alternative would be to investigate further the CLIC beam parameters in order to minimize the disruption, the energy spread and the amount of coherent pairs, while maintaining the peak luminosity at the same level.

5 Conclusion

In this paper, a detailed study of the beam losses along the ILC 20 mrad extraction line was performed, with nominal CLIC colliding beams at the interaction point. Strong beam-beam interactions lead to a significant emittance growth and to the emission of beamstrahlung photons, which can then turn into e^+e^- coherent pairs. All these particles must be transported from the interaction point to their dump, through a post-collision extraction line, with minimal losses. The particle tracking studies that we performed with DIMAD clearly show that the power losses are mostly due to the low-energy tails of the disrupted beams, which are over-focused in the first quadrupoles of the post-collision line. The power deposited by the beamstrahlung photons is negligible. As for the e^+e^- coherent pairs, the power losses are about one order of magnitude smaller than for the disrupted beam. Still, in contrary to lower-energy cases (for instance at ILC with a center-of-mass energy of 500 GeV or even 1 TeV), their contribution can not be neglected at CLIC.

We have shown that the design of the ILC 20 mrad extraction line is not adapted to the nominal CLIC beam, because the power losses are too large (about 280 kW for the disrupted beam and 36 kW for the coherent pairs). A strong reduction of all dipolar and quadrupolar fields allows to bring the power losses down to a reasonable level but, on the other hand, the optics of the extraction line is destroyed at the nominal energy, which prevents from performing measurements of the outgoing beam. A new design must thus be investigated for the CLIC post-collision line, which handles both the low-energy tail of the disrupted beam and the coherent pairs, which carry in average only 10% of the nominal beam energy and which furthermore consist of two types of particles, with opposite charges. Alternatively, one could try to minimize the disruption of the outgoing CLIC beam, its energy spread and the amount of coherent pairs, while maintaining a high luminosity.

Acknowledgements

This work is supported by the Commission of the European Communities under the 6^{th} Framework Programme "Structuring the European Research Area", contract number RIDS-011899.

The author wishes to thank Y. Nosochkov (SLAC) and D. Schulte (CERN) for helpful discussions.

References

[1] The CLIC Study Team, ed. G. Guignard, "A 3 TeV e^+e^- linear collider based on CLIC technology", CERN 2000-008.

[2] I. Wilson, "The compact linear collider CLIC", CLIC note 617, CERN-AB-2004-100, published in Phys. Rep. 403-404 (2004) 365-378.

[3] D. Schulte and F. Zimmermann, "The crossing angle in CLIC", CLIC note 484, CERN-SL-2001-043 (AP), CERN-PS-2001-038 (AE), presented at the 2001 Particle Accelerator Conference, Chicago, USA, June 18-22, 2001.

[4] http://www.interactions.org/linearcollider/

[5] A. Ferrari and Y. Nosochkov, "Beam losses in the extraction line of a TeV e^+e^- linear collider with a 20 mrad crossing angle", EUROTeV-Report-2005-025.

[6] D. Schulte, TESLA-97-08 (1996).

[7] F. Tecker *et al.*, CLIC note 627.

[8] P. Chen, "Coherent Pair Creation from Beam-Beam Interaction", SLAC-PUB 5086 (1989).

[9] R. Arnold, K. Moffeit, Y. Nosochkov, W. Oliver, A. Seryi, E. Torrence and M. Woods, "Design of ILC extraction line for 20 mrad crossing angle", Proceedings of PAC 2005, Knoxville, USA.

[10] http://www.slac.stanford.edu/accel/ilc/codes/dimad

[11] K.L. Brown, D.C. Carey, Ch. Iselin and F. Rothacker, "TRANSPORT, a computer program for designing charged particle beam transport systems", SLAC 91, NAL 91 and CERN 80-04.